Modeling of the Voltage Snap-Back in Amorphous-GST Memory Devices

M. Rudan†, F. Giovanardi†, T. Tsafack†, F. Xiong¶, E. Piccinini†,
F. Buscemi†, A. Liao¶, E. Pop¶, R. Brunetti§, C. Jacoboni§
†Advanced Research Center on Electronic Systems (ARCES) and Department of Electronics (DEIS)
University of Bologna, Via Toffano 2/2, 40125 Bologna, Italy
Phone: +39-05120-93016, Fax: -93073, email: mrudan@arces.unibo.it
§S3 Research Center, CNR—Institute of Nanosciences, and
Physics Department, University of Modena and Reggio Emilia, Modena, Italy
¶Micro and Nanotechnology Lab., University of Illinois at Urbana-Champaign, Urbana IL 61801, USA

Abstract

Charge transport in amorphous chalcogenide-GST used for memory devices is modeled by means of two contributions: hopping of trapped electrons and motion of band electrons. Field-induced emission is accounted for as the mechanism mainly responsible for the trap-to-band transitions. The experimental snap-back behavior of the $I(V)$ curves is reproduced even in the simple case of one-dimensional, uniform structures as the one considered in the paper.

Introduction

Chalcogenide-GST materials can suitably be exploited for manufacturing phase-change memory devices [1]. The principle of chalcogenide memory was first proposed in the late 1960s by Ovshinsky [2]. While crystalline GST exhibits an almost Ohmic $I(V)$ curve, amorphous GST shows a high resistance at low biases whereas, above a threshold voltage $V_{\rm th}$, a transition takes place from a highly-resistive to a conductive state. The transition is characterized by a swift rise in the current, along with a voltage snap-back, leading to an S-shaped $I(V)$ curve. It is useful to remind that the device is current driven, so the experiments actually yield one-valued, N-shaped $V(I)$ curves.

Modeling the threshold behavior is of the utmost importance for exploiting the chalcogenide materials in the fabrication of alternative nonvolatile memories. The model worked out here is a generalization of that presented by some of the authors in an earlier paper [3], where only the hopping processes through localized states [4] —due to a combination of tunneling and thermal excitation— were considered. Here the transport model is enriched by considering a second contribution to conduction due to the electrons occupying extended states, acting in parallel to the contribution of the hopping processes. The model explains the snap-back event even in the simple case in which the device is one-dimensional and spatially uniform. The model includes macroscopic equations incorporating a few parameters and, as shown below, lends itself to fitting experimental data.

Macroscopic Model

Classical concepts like density, average velocity, and current density are used for describing the carrier collective motion. It is convenient to distinguish the density n_T of the electrons that belong to the traps from the density n of the electrons occupying extended states. The latter electrons, here called "band electrons", are free to move along the device and may also undergo scattering processes with the lattice. When this happens they exchange part of their energy with the lattice, without necessarily becoming trapped again. In turn, trapped electrons are able to move from one trap to another by tunnel effect. They may also be scattered by exchanging phonons with the lattice and moving among the localized energy levels of a trap. At equal carrier densities the contribution of the trapped electrons to the conductance is smaller than that of the band electrons. The effects described here are schematically illustrated in figures 1 and 2, that refer to a low-field and high-field condition, respectively. More details are given in the figure captions.

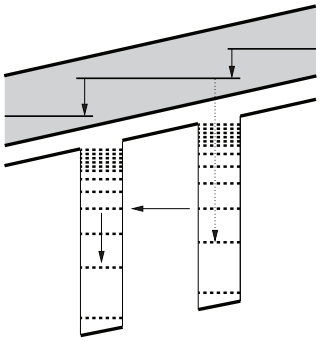

Fig. 1. Schematic description of electron transitions in a low-field case. The distance between the traps is large enough to make the electron wave functions localized within each trap, hence discrete energy states exist. Tunnel transitions between traps occur with low probability (horizontal arrow). Trapped electrons also scatter to different energy states (e.g., vertical arrow in the left trap). A small population of high-mobility electrons belong to the band states (grey region). They exchange energy due to collisions (vertical arrows within the band). The probability that a band electron is scattered back into a trap is small (dotted vertical arrow in the right trap).

Different mechanisms exist that produce the electron transitions from traps to the band. The important ones are impact ionization and field-induced emission. The former is not considered for the devices under investigation because the

978-1-4244-7700-5/10/$26.00 ©2010 IEEE

energy acquired by the band electrons while crossing the device is not sufficient to produce impact ionization. The analysis will then consider field-induced emission only.

In the one-dimensional model used here, spatial uniformity of n_T and n is kept also when a current is flowing. This rules out the diffusive contribution to carrier transport and the formation of electric dipoles, which may be introduced as later refinements of the theory. The need to solve the Poisson equation is ruled out as well, because the electric field $\mathcal{E}$ is constant. As the device is globally neutral, spatial uniformity implies charge neutrality, $n_T+n-N=0$, where $qN > 0$ is the compensating charge density discussed below. The whole device is then described as the series of the amorphous material with conductance

$$G_C = (A/L)\, q\, (\mu_T n_T + \mu_n n)\,, \tag{1}$$

and of a constant resistance R_S due to the heater, crystalline cap, and upper contact, so that the total resistance is

$$R = R_S + 1/G_C\,. \tag{2}$$

The structural details mentioned here are visible, e.g., in [1]; here A and L are the cross-sectional area and length of the amorphous material, q the electron charge, μ_T, μ_n the mobilities of the trapped and band electrons, respectively. As the trapped electrons may move only by tunneling and thermal excitation from a trap to another, one expects that $\mu_T \ll \mu_n$. In equilibrium, n is negligibly small. When a current I is injected into the device, trap-to-band transitions due to field-induced emission add to those induced by phonons, this making n to increase at the expense of n_T. If the device departs more and more from equilibrium, n may become much larger than n_T. As $\mu_T \ll \mu_n$, G_C increases strongly. When all initially-trapped electrons have become band electrons, the value of G_C eventually saturates.

Field-induced emission occurs because the field that is produced by the application of the external current bends the upper edge of the potential-energy profile of the traps. Due to this, a trapped electron has a non-negligible probability to tunnel out of the trap and become a band electron (figure 2). As prior to the tunnel event the trap is electrically neutral, after the event it becomes positively charged. This provides the compensating charge mentioned above. In principle the band electron and the compensating charge belong to different spatial locations. However, similarly to what is typically assumed in the modeling of band-to-band tunneling in semiconductors, the spatial separation is considered negligibly small.

As the field grows the tunneling distance shortens, so the tunnel probability sharply increases. In this way the number of band electrons becomes larger. In contrast with the case of impact ionization, field-induced emission has the same probability of occuring regardless of the trap's position. As a consequence, local uniformity is preserved. As mentioned above, the field-emission probability becomes higher as the electric field increases. On the other hand, the electron trap-to-band transitions make the conductivity to increase, which

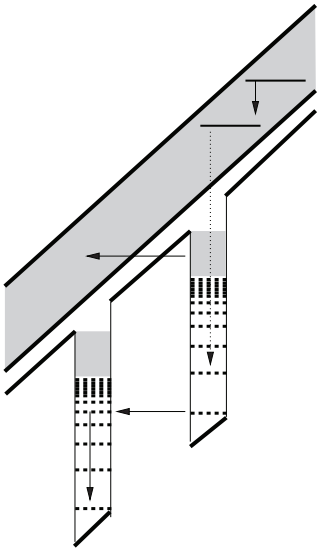

Fig. 2. Schematic description of electron transitions in a high-field case. The distance between the traps is large enough to keep the electron wave functions at lower energies localized within each trap. However, because of the bending of the trap edge due to the external field, the states at higher energies become continuous (grey regions within the traps). The probability of tunnel transitions between traps is still low. Trapped electrons also scatter to different energy states (e.g., vertical arrow in the left trap). The population of high-mobility electrons strongly increases with respect to the low-field case due to trap-to-band tunneling (horizontal arrow from the grey region of the right trap to the band). Band electrons exchange energy due to collisions (vertical arrows within the band). Their probability of being scattered back into a trap is small (dotted vertical arrow in the right trap).

in turn —for a given current— makes the electric field to decrease. The phenomenon thus possesses an intrinsic feed-back mechanism.

Thanks to spatial uniformity the field is uniquely determined by the injected current through the relation $\mathcal{E} = I/(LG_C)$, where the conductance is given by (1). The density of band electrons is written as $n = n_m + (n_M - n_m)\,\sigma(I)$ where the concentrations $n_M \sim N$, $n_m \ll n_M$ are the maximum and minimum value of n (independent of position), and $0 \le \sigma \le 1$ is a dimensionless function (also independent of position) describing the field-emission mechanism. Replacing n and $n_T = N - n$ into the expression of G_C provides $G_C(I)$, namely,

$$G_C = \frac{A}{L}\, q\mu_T N\ (1 + a + b\sigma)\ , \tag{3}$$

with $a \doteq (\mu_n - \mu_T)n_m/(\mu_T N)$, $b \doteq (\mu_n - \mu_T)(n_M - n_m)/(\mu_T N)$ dimensionless parameters. Finally, using

$$V = [R_S + 1/G_C(I)]\ I\,, \tag{4}$$

the $V(I)$ characteristic of the device is found.

Analysis of the Feed-back

The type of feed-back can be described with the aid of figure 3. If the conduction were due to the trap electrons only, the conductance would be low, corresponding, e.g.,

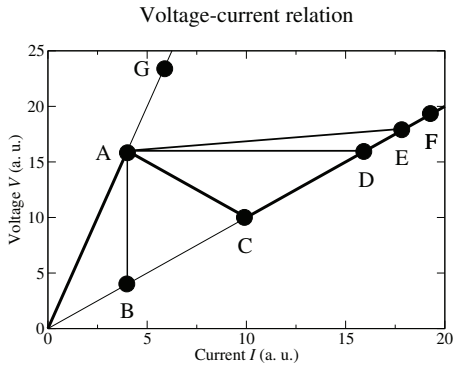

Fig. 3. Schematic voltage vs. current relations used to illustrate the different types of feedback.

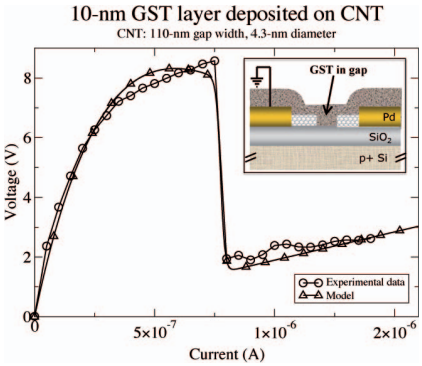

Fig. 4. Fitting of the model to the experimental curve ($T = 295$ K). The device is fabricated as described in [6], and is schematically shown in the inset. The best fit yields $n_M \sim N = 5 \times 10^{18}$ cm^{-3}, $n_m = 10^{-4}N$, $n_M \sim N$, $\mu_n/\mu_{T0} = 20.26$, $I_C = 0.79$ μA, $I_K = 0.01$ μA, $I_F = 0.58$ μA.

to a $V(I)$ relation given by the line from the origin through the points A and G. If the conduction were due to the band electrons only, the conductance would be high, corresponding to a $V(I)$ relation given by the line from the origin through the points $BCDEF$. Actually, the conductance remains low in the current interval from $I = 0$ to the critical current corresponding to point A. Here the device makes a transition to the high-conductance case. The sharpness of the transition determines the type of feedback. The first limiting case is that of an abrupt transition $A \rightarrow BCDEF$. The second limiting case is such that the voltage increase due to the current increase is exactly compensated by the voltage decrease due to the increase of the conductance, $A \rightarrow DEF$. The realistic cases in which the positive feed-back occurs are between the two limiting cases described above. An example of this is the $V(I)$ characteristic that goes from the origin to A, then from A to C, and finally to DEF. The voltage decrease due to the increase of the conductance prevails over the voltage increase due to the current increase. As consequence, the portion of the $V(I)$ characteristic after point A has negative differential conductance, typical of the positive feed-back. Finally, the $V(I)$ characteristics beyond the second limiting case ($A \rightarrow EF$) describe a negative feed-back, where the voltage decrease due to the increase of the conductance is weaker than the voltage increase due to the current increase.

The experiments show that a portion of the $V(I)$ characteristic has a negative differential conductance. As a consequence, the law governing the transitions of the electrons from the traps to the band must depend sharply on the driving force. This is indeed the case of the field-induced emission, as discussed in the next section.

On the other hand, a strong dependence on the driving force does not seem sufficient in itself to make the positive feedback physically possible. In fact, the increase in conductance described above weakens the driving force. This would apparently counteract the emission mechanism and quickly bring the electrons back into the traps. To complete the analysis one must then observe that the typical mechanism by which the band electrons are captured by the traps is phonon scattering. As a consequence, the trap repopulation due to the weakening of the driving force is dominated by a relaxation time which is not related to the emission mechanism. Such a relaxation time is expected to be substantially larger than that of the intra-band collisions. Due to this, a consistent fraction of the electrons emitted from the traps will occupy band states also after the weakening of the electric field, this making the positive feed-back effective. It is worth noting that a similar interplay between the generation and relaxation process had been proposed in [5], where impact-ionization was proposed as the driving mechanism for the negative differential conductance.

Model of the σ Function

To investigate the dimensionless function σ of (3) we use a simplified description in which the emission from a trap into the band is described as the crossing of a barrier of thickness s by an electron of total energy E, where E is lower than the top of the barrier (the schematic representation is in figure 2). The wave function of the electron on the right (left) of the barrier is approximated with the asymptotic limit, namely, by a plane wave with wave vector k_1 (k_2). The transmission coefficient $T(E)$ can be expressed in terms of the fundamental solutions u, v of the Schrödinger equation in the interval $[0, s]$. Using the boundary conditions $u(0) = 1/v'(0) = u_0$, $v(0) = u'(0) = 0$, where u_0 is an arbitrary non-zero constant, and using the index s to indicate the values at $x = s$, one finds

$$\frac{1}{T} = \frac{1}{2} + \frac{(u_s')^2 + (k_2 u_s)^2}{4u_0^2 k_1 k_2} + \frac{(v_s')^2 + (k_2 v_s)^2}{4k_2/(u_0^2 k_1)}\,. \qquad (5)$$

The transmission coefficient depends on E through the wave vectors and the values of the fundamental solutions at $x = s$, which in turn depend on the form of the potential energy in the interval $[0, s]$. Although the latter information is not available, one may assume that the dependence of

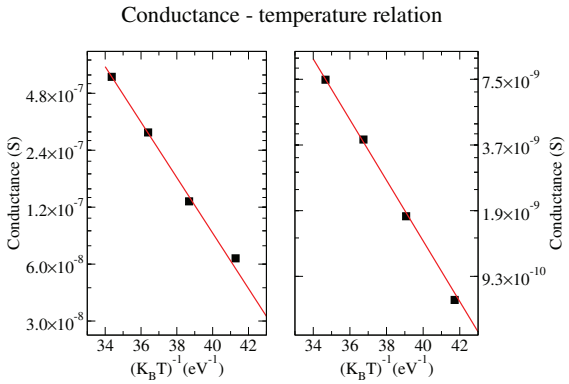

Fig. 5. Comparison of the conductance dependence on temperature with two sets of experimental data taken from ref. [7], left, and ref. [6], right. The different conductances are related to the experimental conditions; the parameter E_a is 0.33 ± 0.01 eV in both cases.

the fundamental solutions on s and E is exponential-like because the electron energy E is lower than the top of the barrier. For instance, in case of a square barrier whose top energy is V_0, the fundamental solutions at $x = s$ are $\cosh(\alpha s)$, $\sinh(\alpha s)$, with $\alpha = \sqrt{2m\,(V_0 - E)}/\hbar$.

The external field is due to the current injected into the device. It is sensible to assume that in the trap region the voltage drop due to the current injection has a much smoother dependence on position than that of the barrier that surrounds a trap. As consequence, when the external field is modified by a change in the injected current, the variation in the parameters k_1, k_2, $u_s \ldots$ of (5) acquires an exponential-like dependence on the field or, equivalently, on the current. Such a dependence is kept when the contributions of the different energy levels E are summed up. In this paper, due to the lack of detailed information about the form of the potential energy in the trap region, the approximate expression $\sigma = \{1+\exp[(I_C - I)/I_K]\}^{-1}$ has been adopted, with I_C, I_K parameters. The first one is the value around which the snap-back occurs, while the second one determines the extent of the snap-back region.

Results

The $V(I)$ relation found by the present model is N-shaped, this corresponding to the expected snap-back behavior of the $I(V)$ curve. However, the slope of the curve before the snap-back is everywhere linear. In fact, taking $\sigma \sim 0$ reduces (1) to $G_C \simeq (A/L)\, q\mu_T N$, which makes the slope of the $V(I)$ relation (4) a constant. This outcome is in contrast with the experimental evidence. In fact, the latter shows that the low-current branch is linear only near the origin, whereas at relatively higher currents it exhibits an exponentially-increasing behavior (figure 4). The model must then be improved. Observing that at low currents the band electrons do not practically contribute to the transport, the model is modified by making the mobility of the trap electrons to increase with the electric field. This is consistent with the description of the motion of such electrons as due to hopping between traps. In fact, if the field is not high enough to make the trap-to-band transition possible, an increase in the field makes the trap-to-trap hopping easier, hence the mobility μ_T becomes larger.

The mobility field-dependence due to this effect is of exponential type. As above, it is more convenient to initially express the dependence in terms of the current, and later convert it to a field dependence. Namely, $\mu_T = \mu_{T0} \exp(I/I_F)$, $I \geq 0$, with I_F a parameter.

The model has been tested against experimental data. GST layers have been deposited using the method shown in [6], which makes use of carbon nanotubes (CNTs) as electrodes. In order to obtain the two electrodes, a Joule breakdown of CNTs exposed to ambient air is induced. This creates a gap in between the CNTs. Next, the GST is sputtered to refill the gap and cover the CNTs. A schematic of the device is reported in the inset of Fig. 4. This procedure ensures that the GST in the gap is initially amorphous, as testified by very high resistance found in $V(I)$ characteristics. An example of the fitting is shown in figure 4, demonstrating a fair agreement despite the sharpness of the snap-back transition. The quality of the fitting at different temperatures and size of the samples is similar.

Another feature of the model is the agreement of the temperature dependence of G_C with the experiments (figure 5). To discuss this aspect it is convenient to use (1) in the form $LG_C/(qA) = \mu_T N + (\mu_n - \mu_T)n$. In the equilibrium condition the electrons distribute in the energy states according to the Fermi statistics and, if the temperature T_L becomes larger, the concentration n of the band electrons increases as well. As the dependence of n on T_L is much stronger than that of the mobilities, it follows (assuming for simplicity a non-degeneracy condition) $G_C(T_L) = A + B \exp[-E_a/(k_B T_L)]$, with k_B the Boltzmann constant and A, B, E_a parameters. This provides a sensible indication supporting the existence and nature of the extended states in the material.

Acknowledgement

Part of the work has been carried out under the contract 34524/2009 of the Intel Corporation, whose support is gratefully acknowledged.

References

[1] D.C. Kau et al., *A stackable cross point phase change memory*, Proc. IEDM09, p. 617–620 (2009).

[2] R.S. Ovshinsky, *Reversible electrical switching phenomena in disordered structures*, Phys. Rev. Lett. **21**, 1450–1453 (1968).

[3] F. Buscemi et al., *Monte Carlo simulation of charge transport in amorphous chalcogenides*, J. Appl. Phys. **106**, 103706 (2009).

[4] N.F. Mott, E.A. Davis, *Electronic processes in noncrystalline materials*, Clarendon Press, Oxford (1961).

[5] D. Adler et al., *Threshold switching in chalcogenide-glass thin films* J. Appl. Phys. **51**, 3289 (1980).

[6] F. Xiong et al., *Ultra-low power phase-change memory with carbon nanotube interconnects*, Proc. DRC (2010).

[7] D. Ielmini and Y. Zhang, *Evidence for trap-limited transport in the subthreshold conduction regime of chalcogenide glasses*, Appl. Phys. Lett. **90**, 192102 (2007).